Title: Sickle cell patients showed dysregulated plasma Rb/K ratio and Gamma-glutamyl cycle in red blood cells

Author (s): Shruti Bhatt[1], Amit Kumar Mohapatra[2], Satyabrata Meher[3], Apratim Sai Rajesh[4], Pradip Kumar Panda[4], Ranjan Kumar Nanda[2*] and Suman Kundu[1,5*]

[1]Department of Biochemistry, University of Delhi South Campus, Delhi, India
[2]International Centre for Genetic Engineering and Biotechnology, New Delhi 110067
[3]Sickle Cell Institute, Veer Surendra Sai Institute of Medical Science and Research, Sambalpur, Odisha, India
[4]Sri Sri College of Ayurvedic Science and Research, Sri Sri University, Cuttack, Odisha, India
[5]Biological Sciences, Birla Institute of Technology and Science–Goa, India

***Correspondence:**
Prof. Suman Kundu
Director, BITS Pilani, K.K.Birla Goa Campus
Professor Department of Biochemistry (on lien)
DU, South Campus
New Delhi, India
Telephone No: +91 9899007460
Email address: suman.kundu@south.du.ac.in; skundu@goa.bits-pilani.ac.in
Dr. Ranjan Kumar Nanda
Group Leader
Translational Health Group
International Centre for Genetic Engineering and Biotechnology, New Delhi 110067
Email address: ranjan@icgeb.res.in

Running title: RBC metabolome in sickle cell disease

Abstract

Patients suffering from Sickle cell disease (SCD) present with multifactorial pathology, and a detailed understanding of it may help to develop novel therapeutics. In this study, the plasma elemental (^{24}Mg, ^{44}Ca, ^{57}Fe, ^{63}Cu, ^{66}Zn, ^{77}Se, ^{85}Rb, ^{208}Pb, and ^{39}K) levels of SCD patients (n=10, male: 50%) and control groups (trait and healthy; n=10 each; male: 50%) were profiled using inductively coupled plasma mass spectrometry (ICP-MS). Additionally, comparative global erythrocyte metabolomics of SCD (n=5, male:100%) and healthy controls (n=5, male:100%) were carried out using liquid chromatography-mass spectrometry (LC-MS). SCD patients had higher plasma ^{24}Mg, ^{44}Ca, ^{66}Zn, ^{208}Pb, and ^{39}K levels and lower levels of ^{57}Fe, ^{77}Se, and ^{85}Rb compared to controls. These changes in elemental levels with a decreased Rb/K ratio, may explain the observed frequent hemolysis and severe dehydration with oxidative stress in the SCD group. Mass spectrometry analysis of RBCs (red blood cells) of SCD (n=5) and healthy controls (n=5) identified 442 unique metabolic features which separately clustered both the study groups in principal component analysis (PCA). A set of 136 features showed differential ($p<0.05$; $\log_2$fold change$>\pm1$) regulation and was involved in D-Glutamine/D-glutamate, Sphingolipid, Arginine biosynthesis, Glutathione and Glycine, serine and threonine metabolism. Interestingly, higher pyroglutamic acid levels were observed in the SS-RBCs (sickle shaped-RBC) indicating a perturbed gamma-glutamyl pathway in SCD patients. Supplementation of the depleted trace metals and targeting the perturbed metabolic pathways in the RBCs of SCD patients provides avenues for alternate therapeutics development.

Key words: sickle cell disease; metabolomics; ionomics; red cells; oxidative stress; mass spectrometry.

Graphical abstract

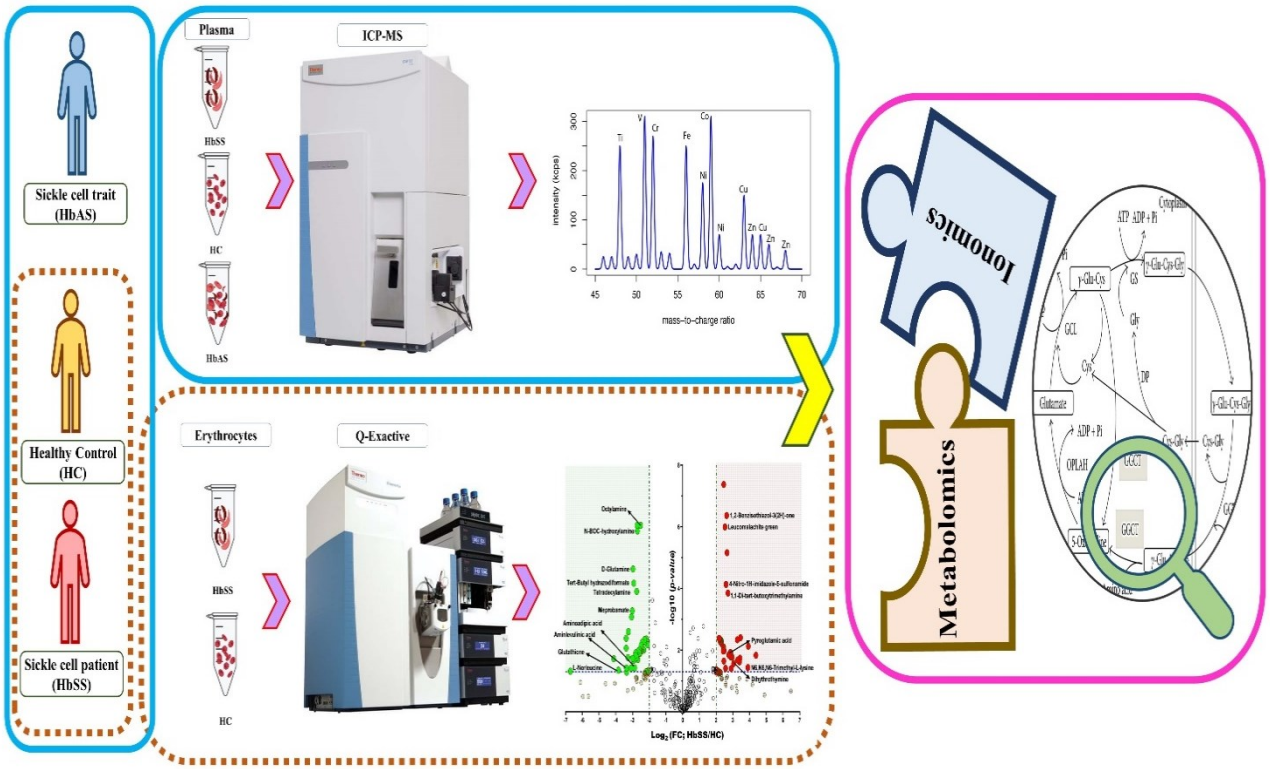

1. Introduction

WHO has recognized Sickle cell disease (SCD), the first known molecular disorder, as a global health pandemic. SCD cases are predicted to increase from 300,000 to 400,000 by 2050 and the majority (2/3) of it was recorded in Africa and India [1-5]. SCD is caused by a genetic mutation that translates into the substitution of Valine in place of Glutamic acid, at the 6th position in the β chain of the hemoglobin molecule leading to a structural variant as Hemoglobin S (HbS) [6-8]. HbS has a reduced oxygen affinity, and deoxygenation near tissues leads to exposure of hydrophobic sites on individual T-state HbS molecules [9].

Exposed hydrophobic sites act as a nucleus on the HbS molecule, aggregating and forming a 14 nm fiber leading to the Sickle Shaped RBCs (SS-RBCs). SS-RBCs block the blood vessels leading to an impaired blood supply to organs causing recurrent episodes of acute pain (vaso-occlusive crisis: VOC) and chronic damage leading to poor survival [10-14]. Understanding the detailed pathophysiology of SCD at the molecular and elemental level will be useful to identify targets for better clinical management [15].

Limited reports have shown the perturbed metabolic pathways and elemental levels in SCD patients [16-19]. Multi-omics studies using liquid chromatography and inductively coupled plasma mass spectrometry (LC-MS/ICP-MS) are useful to capture the metabolites and elemental details to better understand the disease pathophysiology.

In this study, a comparative plasma elemental composition was monitored between SCD and control (traits and healthy) groups and global RBC metabolome profiling between SCD and healthy controls was performed. The lack of validated biomarkers for SCA severity represents a void in the state of knowledge of SCD that creates a critical roadblock in the design of clinical trials, the development of novel therapies and the emergence of precision medicine for SCD patients.

2. Materials and Methods

2.1 Ethics statement

All participants provided informed consent before participating in the study. This study was approved by the Institutional ethics committee of Sri Sri University, Cuttack, Odisha (SSCASRH/IEC/006/21) and University of Delhi South Campus, Delhi, India (UDSC/IEC/2021/Project/5.10.2021/4). The human studies reported in this study abide by the Declaration of Helsinki principles.

2.2 Study participants

For this study, blood samples were collected from a cohort of ten adult SCD patients with hemoglobin SS (HbSS, n=10, male 50%) disease (Table S1), sickle cell trait individuals (hemoglobin AS: HbAS, n=10, male 50%) and ten healthy adults (controls, HC, n=10, male 50%). Written informed consent was obtained from all patients and controls. All protocols and procedures were approved by institutional ethics committees of the partnering institutes.

2.3 Sample collection and processing metabolomics

For this study, blood samples were collected from SCD patients in EDTA with hemoglobin SS disease and healthy adults (controls). Complete blood count determined the clinical profile of participants (CBC), cellulose electrophoresis, PCR, and HPLC is shown in Supplementary Tables 1 and 2. The participants were enrolled according to inclusion and exclusion criteria with consent (S.1.2). The inclusion criteria were a confirmed diagnosis of sickle cell disease by HPLC. Individuals who had received a transfusion were excluded from the study. All patients were receiving analgesic treatments. Blood samples, taken from patients with SCD, were characterized by their sickling properties [20]. Blood tubes were then centrifuged at 2000 ×g for 10 min to separate the RBCs and plasma and were aliquoted into equal volumes (0.5 ml) and for stored until the analysis. Plasma samples were stored in a –80 °C freezer until analysis. Samples were processed according to a biphasic liquid-liquid extraction (LLE) protocol.

Briefly, RBC metabolism was quenched by extracting metabolites into methanol/water/chloroform solvents.

2.3.1 Untargeted metabolite profiling of sickle RBCs

The 0.5 ml aliquots of human donor erythrocytes (Sri Sri University) that had been pre-treated with heparin anti-coagulant were placed in 2.0 ml microcentrifuge tubes (MCT). After adding internal standards, they were centrifuged at 1000 ×g and 4 °C for 2 min, then placed on ice while the supernatant was aspirated. The RBCs were washed twice with their resuspension in 1x phosphate-buffered saline (PBS) through centrifugation, and finally the supernatant was aspirated to leave an RBC pellet. These wash cycles remove non-erythrocytic metabolites and other compounds that may still be present outside the cells; however, it also delays quenching, and might leave residual traces of phosphate salts.

2.3.2 Metabolite Extraction

To the RBC pellet of each tube, 0.15 mL of ice-cold, ultrapure water (Milli-Q Millipore, Mississauga, Canada) was added to resuspend the erythrocytes. The tubes were first plunged into the dry ice for 30 seconds followed by 20 seconds of incubation in the water bath at 37 °C to quench metabolism and lyse the cells. After quenching with dry ice, 0.6 ml of methanol at 20 °C temperature was added, and the tubes were then vortexed to ensure complete mixing. The tubes were then again into dry ice where 0.45 ml of chloroform was added to each tube. These tubes were vortexed briefly every 5 min for 30 min, and between each brief vortexing interval, they were placed in a cold bath. After 6 brief vortexes the tubes were transferred to room temperature and 0.15 ml of ice-cold, ultrapure water (Milli-Q Millipore, Mississauga, Canada) was added to drive the phase separation between methanol and chloroform. The tubes were centrifuged at 1,000 ×g for 2 min at 4 °C so a clear separation of the two phases could be observed above and below the compact disk of erythrocytes. After centrifugation, the tubes were transferred to a –20 °C freezer for an overnight incubation to allow residual chloroform to precipitate out of the aqueous methanol phase. The two liquid phases in each tube were transferred to separate 1.5 mL microcentrifuge tubes without disturbing the compact disk of erythrocytes or transferring any erythrocytes to the new tubes. The final volumes translated to a methanol/water/chloroform ratio of 4:2:3 for extraction and phase separation. The samples were then dried with speed-vac and resuspended in 0.2 mL LC mobile phase (97.9% ultra-pure water / 2% acetonitrile / 0.1% formic acid).

2.3.3 UPLC-Q-Exactive Plus Orbitrap MS/MS Analysis

Liquid Chromatography: All the samples were analyzed using an Ultimate 3000 UPLC system (Dionex, United States) that was controlled with Thermo Xcalibur software (Thermo Fisher Scientific, United States). The samples were separated using a Kinetex UPLC C18 column (100 × 2.1 mm, 1.9 µm; Phenomenex, Torrance, CA, United States). The mobile phase consisted of solvent A (0.1% formic acid) and solvent B (acetonitrile with 0.1% formic acid). Gradient elution was applied using the following optimized gradient program: A 35-min gradient at a flow rate of 0.3 ml/min with the following conditions was used for separation: 0–5 min, 1% B; 5–10 min, linear gradient from 1–3% B; 10–18 min, linear gradient from 3–40% B; 18–22 min, linear gradient from 40–80% B; 22–27 min, column cleaning at 95% B; and 27–35 min, re-equilibration at 1% B.

Mass spectrometry was performed on a Q-Exactive Plus™ quadrupole-Orbitrap mass spectrometer (Thermo Fisher Scientific, United States) in positive ion mode. Data-dependent acquisition method was used for MS/MS of small molecules in the extractions. The complete MS settings were 70,000 resolution, 1e6 AGC, 100 ms max inject time, and 100–1500 m/z. The MS/MS settings were 35,000 resolution, 1e5 AGC, 100 ms max inject time, 1.0 m/z isolation window, and 30 dynamic exclusions. Three technical replicates were run for each extraction, and each technical replicate used a different HCD collision energy (25, 30, and 35, respectively).

Compound Discoverer™ 3.0 (Thermo Fisher Scientific, United States) software was used to analyze the LC-MS/MS data for each extraction in positive ion mode.

Data normalization and analysis were carried out using MetaboAnalyst 5.0 (www.metaboanalyst.ca) [21]. Data exclusion was performed for metabolites with constant values across metabolites and interquartile filtering. Missing values were mean imputed, and normalization was performed using log10 transformation. For univariate analysis, fold changes and T-test values were calculated, then multiple testing correction was performed based on false discovery rate (FDR). ROC-curve analysis was also carried out for each metabolite, and 95% confidence intervals were calculated using bootstrapping with 500 permutations. Multivariate exploratory analysis was performed using principal component analysis (PCA) and orthogonal projections to latent structures discriminant analysis (OPLS-DA), as implemented in MetaboAnalyst. Permutation testing for OPLS-DA was applied to evaluate model stability to parameter addition. Linear support vector machine (SVM) classifiers were built to predict group class using Monte-Carlo cross-validation (MCCV) and balanced subsampling. Six SVMs with an increasing number of metabolites (maximum 100) were compared. Model evaluation was performed using ROC curves, and biomarker identification was achieved using the feature ranking method implemented in SVM (S.2.2, Fig. S3a, b, c).

2.4 Trace metal quantification using inductively coupled plasma mass spectrometry (ICP-MS)

Plasma samples of study groups were processed and subjected to ICP-MS to quantify ^{24}Mg, ^{44}Ca, ^{57}Fe, ^{63}Cu, ^{66}Zn, ^{77}Se, ^{85}Rb, ^{208}Pb, and ^{39}K. Plasma samples (100 µl) were transferred to MG5 vials (Anton Paar), and HNO_3 (250µl, 70%, #225711 Sigma Aldrich, ≥99.999% trace metal basis) and H_2O_2 (50µl, 30%, 231 #1.07298.1000, Supelco.) were added. Vials were sealed using sealers (#411860, Anton Paar). The vials containing the reaction mixtures were digested using a microwave digestion system (Anton Paar) ramped up to 300 W in 15 min, where it was held for 10 min. The digested samples diluted using trace metal-free water (18.2 MΩ×cm) for inductively coupled plasma mass spectrometry (ICP-MS) analysis. Digested samples were analyzed using ICP-MS (iCAP™ TQ ICP-MS, Thermo Scientific, USA). Thermo Scientific Qtegra Intelligent Scientific Data Solution (ISDS) software was used for operating and controlling the instrument. The ICP-MS was calibrated using a multi-element standard mix (#92091, Sigma Aldrich) prepared in 1% HNO_3 per the manufacturer's instruction. Calibration plots were prepared at 1 ppb to 5 ppm concentrations and showed R^2= 0.99. Digested samples were aspirated using a V-grooved MicroMist DC nebulizer and spray chamber of ICP-MS using a sample capillary (0.55 mm). Samples were then passed through a quartz torch with an injector having a diameter of 2 mm. Here, plasma ionized samples passes through sample cones, followed by a skimmer cone. The experiment was conducted in KED (Kinetic energy dissociation) mode to avoid any polyatomic ion interference. During the run, the nebulizer flow was set at 1.04 l/min with a pressure of 3.20 bar. The peristaltic pump revolved clockwise at 40 rpm. The quartz torch produces plasma and the exhaust was maintained at 0.49 mbar. Interface temperature was maintained at 29.98°C with a N_2 flow of 14 l/min. The system's sample and skimmer cones were made of nickel with orifices of 1 mm and 0.5 mm, respectively. Between sample runs, HNO_3 (1%) was pumped through the nebulizer with a wash-out time of 30 sec to remove any carryover. The complete experiment was carried out with a dwell time of 0.1s. The average of three runs for each element concentration was calculated and exported for further statistical analysis. Comparative trace element levels between study groups (HbSS, HbAS and HbAA) were calculated considering the limit of detection and dilution factors.

2.4.1 Statistical analysis

An unpaired t-test was performed using Graphpad prism 8 to find group-specific variations and a $p<0.05$ was selected as significant.

3. Results

3.1 Clinical Characteristics of the Studied Population

In this case and control study, a total of 30 study participants belonging to SCD as case and control (Sickle cell trait and healthy controls) were used for plasma ionomic and RBC metabolomic profiling. The demographic and clinical characteristics of study participants are presented in Supplementary Tables S1 and S2.

3.2 Sickle cell anemia is associated with an altered ionomic profile

From the comparative plasma trace element analysis, significantly higher plasma levels of Mg ($p<0.0001$), Zn ($p<0.0001$), Ca ($p<0.01$), Pb ($p<0.01$), and K ($p<0.01$) were observed in SCD patients compared to healthy controls (Fig. 1a, c, d, e, h). Significantly lower plasma levels of Fe, Se ($p<0.05$), and Rb ($p<0.01$) were observed, indicating higher oxidative stress in SCD patients (Fig. 1b, g and i). However, Cu levels were similar between study groups (Fig. 1f). Overall, the sickle cell trait subjects had comparable trace metal levels to the healthy controls except for Rb whose levels hovered in between the levels observed in SCD and healthy control (Fig. 1i). We found that there was a steady decrease in Rb/K levels in the SCD group compared to the healthy controls (Fig. 1j)

3.3 Metabolomics profiling of RBCs of SCD patients' showed significant deregulation compared to the healthy controls.

Global metabolomic profiling of RBCs from SCD patients and healthy donors yielded 442 metabolite features. Principal Components Analysis (PCA) analysis of these analytes showed separate non-overlapping clusters of SCD and healthy groups. The principal components 1 and 2 explained 44.2% of the total variance (Fig. 2a). A supervised OPLS-DA model was evaluated to identify significant differentially abundant metabolites between groups and validated using permutation tests (Fig. S2a). A random permutation test ($n = 2000$) resulted in an interpretation rate (R_2) and prediction ability (Q_2) of 0.999 and 0.891, respectively (Fig. S2b). A set of 10 analytes (S.2.2, Fig. S2c) qualified the variable importance in projection (VIP) scores >1.0 and were identified as important metabolites. These metabolites displayed significantly different concentrations between groups, with fold changes >1.0 or <0.5. In the univariate analysis, 136 showed differential expression (62/56; up-/down-regulated; FC>; $p<0.005$) in SCD (Fig. 2b, Table S3 and Table S4). After false discovery rate adjustment, 18 analytes (7/10; up/down regulated) showed significant deregulation. In the RBC of SCD patients, Glutathione, Aminolevulinic acid, DL-2-Aminooctanoic acid, D-Glutamine, and Aminoadipic acid (Table S3) levels were significantly high. Significantly lower levels of N6,N6,N6-Trimethyl-L-lysine, Dihydrothymine, Pyroglutamic acid, 2'-alpha-mannosyl-L-tryptophan and 2-Aminoisobutyric acid were observed in the RBC of the SCD patients compared to healthy controls (Fig. 2b, 2c). Hierarchical clustering analysis was performed to identify top 25 significantly dysregulated metabolic features in SCD and healthy control (Fig. 2c).

Functional pathway analysis

The significantly dysregulated metabolites in SCD group were selected for the KEGG pathway analysis using MetaboAnalayst. D-Glutamine and D-glutamate metabolism (p-value = 0.0006, Fig. S6a), Aminoacyl-tRNA biosynthesis metabolism (p-value = 0.0009), Sphingolipid metabolism (p-value = 0.0009), Arginine biosynthesis (p-value = 0.00099), Glycine, serine and threonine metabolism (p-value = 0.004, Fig. S6b), beta-Alanine metabolism ($p<0.005$), Arginine and proline metabolism ($p<0.007$), Glutathione metabolism ($p<0.009$, Fig. S6c), Glutathione metabolism ($p<0.01$), and Ether lipid metabolism ($p<0.012$) were significantly altered in the RBC of SCD patients compared to the control group (Fig. 2d).

4. Discussion

The overwhelming significance of RBCs stems from the enormous abundance of hemoglobin. Any alteration in structural and functional attributes of hemoglobin can translate into irregularities in RBC functions. These irregularities can have different clinical complications

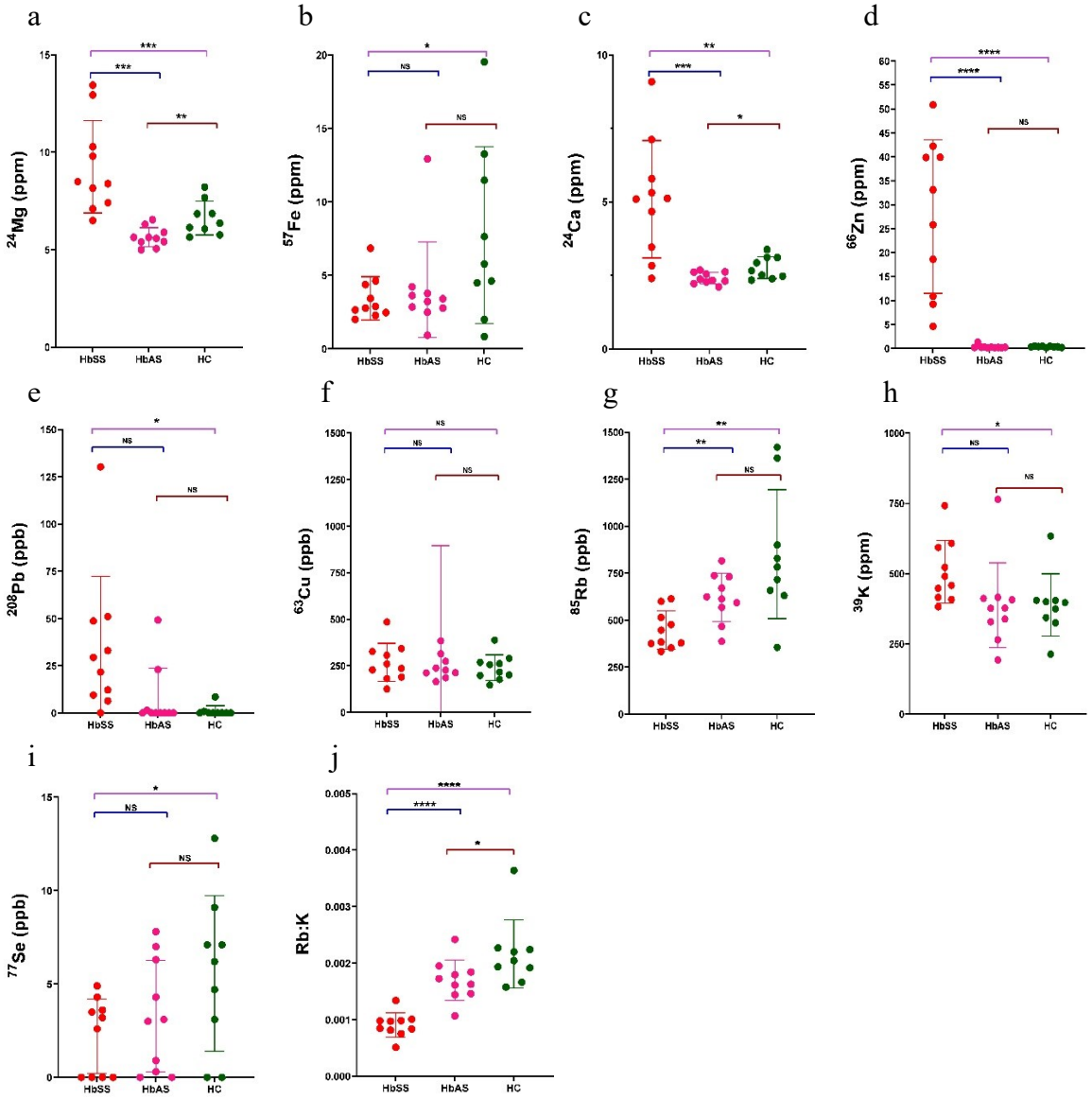

Figure 1. Plasma trace element levels of Sickle cell patient (HbSS), sickle cell trait (HbAS) and healthy control (HC) and their ratio showed significant differences. a) Mg, b) Fe, c) Ca, d) Zn, e) Pb, f) Cu, g) Rb, h) K, i) Se, j) Rb:K. *$p < 0.05$, **$p < 0.01$, ***$p < 0.001$ **** $p < 0.0001$; HbSS: Sickle cell disease; HbAS: Sickle cell trait; HC: Healthy control.

inside the human body [22-24]. The RBCs are designated as a simple model to study cellular mechanisms due to less epigenetic, transcriptional and translational complications to regulate the cross-talk amongst various pathways [25-27]. However, recent omics studies highlight the existence of a complex network of cytosolic enzymes which regulate the energetics and functioning of RBCs [28, 29]. Physical and pathological stresses can alter the metabolic equilibrium and accelerate disease progression. Thus, an in-depth understanding is required to deconstruct the highly interlinked stressed RBC pathophysiology [30].

Enhanced hemolysis observed in SCD patients might be contributing to the observed higher plasma magnesium level ($p<0.001$) [31]. This finding is in agreement with observations by Olukoga, A. O et al. (1990) [32] which establishes a negative correlation between erythrocyte

magnesium and plasma magnesium in the SCD cohort [33]. In contrast, low serum magnesium levels have been reported in SCD patients due to Mg homeostasis [34, 35].

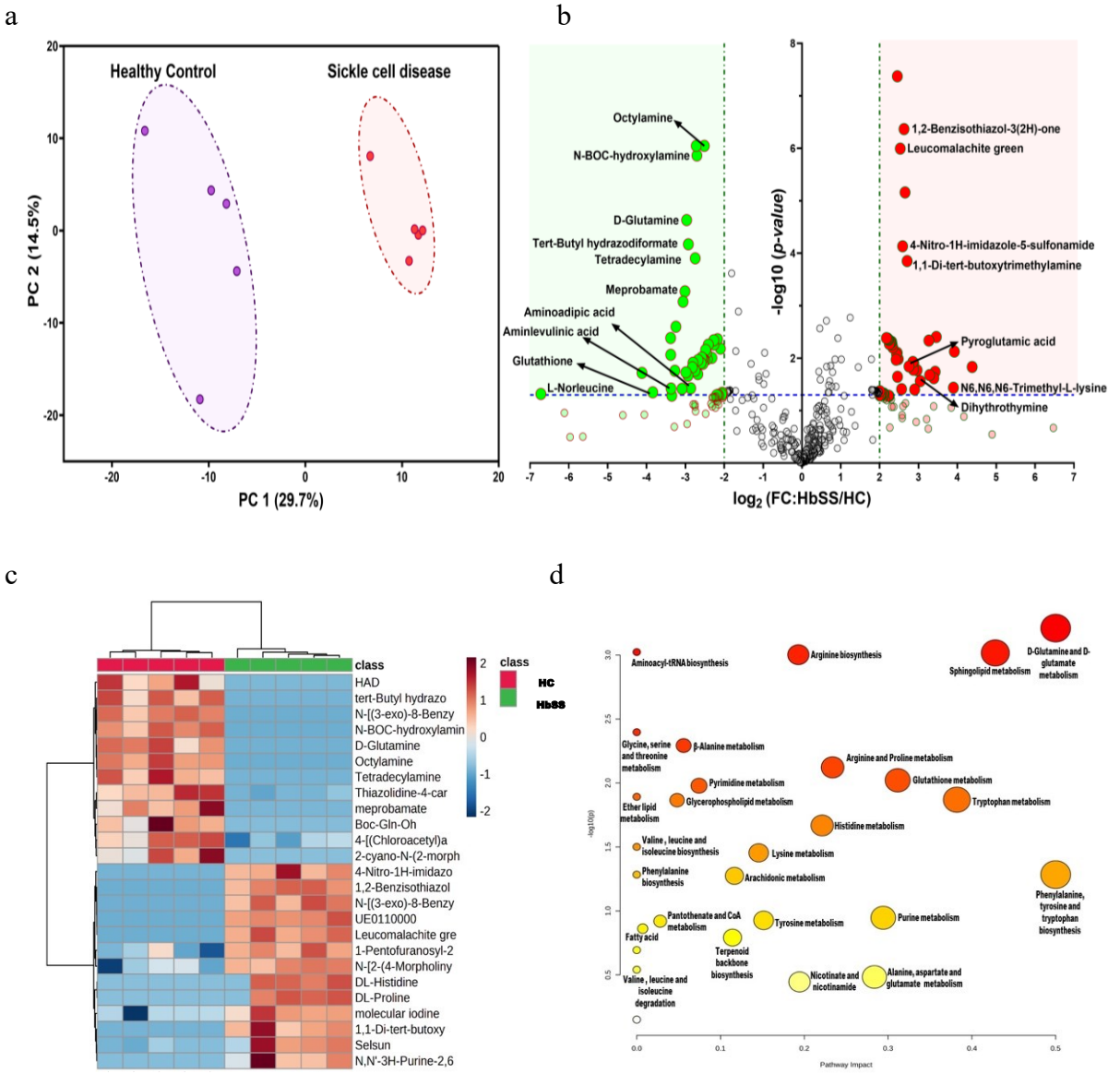

Figure 2. Pertubed RBC metabolic fingerprint observed in sickle cell disease patients (HbSS) compared to the healthy control (HC). a) PCA score plot showed RBC metabolites (n=442) of SCD patients cluster away from the healthy controls. b) Volcano plot highlighting the dysregulated erythrocyte metabolites in SCD (HbSS) compared to the healthy control (HC). c) Hierarchical Clustering showing the distribution of 25 important RBC metabolites in SCD patients and healthy controls. Columns correspond to samples, and rows to individual metabolites. The color scale indicates the relative abundance of metabolites: red being the most abundant and blue the less abundant metabolites. d) Metabolic pathways altered in the RBCs of SCD patients compared to healthy controls. The pathway impact values (x-axis) represent the influencing factor of topological analysis, and the –log(p) (y-axis) represents the p-value of the pathway enrichment analysis. The vital metabolic pathways were defined as having –log(p) > 2 and pathway impact factor > 0.2.

Similarly, RBCs contain 10-15% of the total cellular pool of calcium. Sickle cells show increased calcium as compared to normal cells in the oxygenated state [36]. Malinovská V et al. reported that stress conditions increase plasma Ca levels. Higher plasma calcium levels as observed in SCD patients can be attributed to frequent hemolysis due to prolonged stress in

SCD patients [37]. However, in SCD an accumulation of intraerythrocytic Ca has been reported due to malfunction of $Ca2^+$ transporters [38]. Higher plasma calcium levels as observed in SCD patients can be attributed to frequent hemolysis due to prolonged stress in SCD patients [39]. An increased intracellular calcium concentration induces alteration to calcium-sensitive potassium (K^+) channel protein 4 (also known as the putative Gardos channel) and K–Cl cotransporter 1 (KCC1), KCC3 and/or KCC4 [40], resulting in potassium-efflux and decreased cell volume [41-43], which in turn increases the stiffness of RBC. Similarly, we also observed higher plasma K levels corroborating earlier reports [44-48]. Thus, K^+ is an important indicator of SCD, however, its measurement to assess the severity in many pathophysiological conditions can be erroneous due to factors like pseudohyperkalemia and poses a challenge [49].

Another similar group I alkali metal, rubidium (Rb^+) was significantly lower ($p<0.01$) in SCD patients compared to the trait and control group. It shares similar biochemical properties and readily exchanges with K^+, thus, can be a useful proxy for K^+. Although its biological function still needs further understanding, ^{86}Rb's prominent presence was utilised to measure basal metabolic rate, establishing a correlation between its radioactive turnover and K^+ concentration[50]. We are the first to report a correlation between plasma Rb and K+ concentration which significantly decreased from healthy to trait and even decreased further in the SCD group. Rb may have the potential to be used as a marker to assess the severity associated with sickling. Rb has unique neurophysiological and neuroprotective properties [51-53]. Kordjazy et al. found that mice administered with Rb showed less depression-like behaviour through changes in the hippocampus [54]. Recent clinical trials and studies have widely reported that SCD patients suffer from neuro-cognitive complications [55-57]. Neurocognitive impairment have been reported children with SCD which affects their visuo-spatial memory(14.8%), IQ (85.4%) and copying (68.2%) [56, 58, 59]. These studies indicate that SCD can lead to the development of neuro-complications. Thus, Rb's beneficial role in improving SCD patients' neurocognitive complications can be further explored.

We observed significantly higher plasma lead levels in SCD compared to the trait and healthy cohort. These findings align with previous studies which have correlated BLL levels with moderate and severe anemia [60]. In addition to neurological toxicity, lead can worsen sickle cell anemia by impairing heme synthesis and increasing the rate of red blood cell destruction [61]. Schwartz et al showed a dose-dependent increase in anemia in children with blood lead levels near 25 μg/dl [60, 62]. A linear decrease in hemoglobin was reported in children with increased BLL (BLL >30 μg/dl) by Drossos et al. [63].Although these findings indicate a relationship between lead levels and SCD, a more detailed analysis is required to solidify these claims.

High plasma Zn levels of the SCD group was observed compared to trait and control group which does not corroborate with earlier reports [64, 65]. An increased iron concentration in the intestinal lumen may antagonize the uptake of Zn [66]. Zinc concentrations have been inversely correlated to Copper (Cu) levels [64, 67]. This depletion of Cu could impair iron absorption [68]. However, no such relationship was observed in our present study and no significant change in Cu levels was observed across the group. On the contrary, a steady iron (Fe) increase was observed in trait and healthy group ($p<0.05$) which indicates disrupted Fe homeostasis and most often due excessive urinary loss of iron as reported by some studies [69, 70].

Selenium is an essential component of mammalian enzymes like glutathione peroxidases (GPx) [71, 72], providing antioxidant defence against ROS. Erythrocytes of selenium-deficient rats failed to protect the hemoglobin from oxidative damage in the presence of ascorbate or H2O2 or glutathione [72]. Se deficiency is known to alter erythroid parameters like RBC, HCT, HGB, and MCHC ($P < 0.05$) and makes erythrocytes osmotically fragile [73]. The family is involved in oxidoreduction reactions and these reactions occur in diverse tissues and physiological

445 pathways. Selenium supplementation has preventive and therapeutic role in diverse disease
446 conditions [74-78]. Plasma Se levels were highest in the healthy and lowest in the SCD group
447 ($p<0.05$) so Se supplementation may be beneficial to SCD patients.

448 **4.1 Metabolic insights in sickle RBCs indicate an altered Gamma-Glutamyl cycle which**
449 **fuels ATP depletion from sickle red blood cells**

450 The main oxidative damage control system in RBCs, the glutathione pathway, has been
451 reported to be altered in HbS red blood cells [79]. There is increasing evidence that this
452 alteration leads to oxidative stress which has a negative domino effect on the pathophysiology
453 of SCD [80]. ROS can be derived non-enzymatically (Fenton chemistry) from denatured sickle
454 hemoglobin (Hb S) moieties and lipid peroxidation or derived enzymatically by the action of
455 NADPH oxidase. ROS damage RBC membranes and decrease cell deformability which
456 contributes to the pathophysiology of SCD [81]. Plasma-free hemoglobin (Hb) and iron
457 chelates are by-products of hemolysis that can also act as oxidants [82]. To counteract ROS,
458 mammalian cells have antioxidant pathways involving reduced glutathione (GSH), NAD(H),
459 NADP(H), glutamine and nitric oxide (NO), which are complex and interlinked. Glutathione
460 exists in a reduced (GSH) and oxidized (GSSG) form. The thiol reductant, GSH, scavenges
461 ROS such as hydrogen peroxide and lipid peroxides [82, 83]. GSH can also interact with Hb
462 to form glutathiol-hemoglobin (G-Hb) which reduces the propensity for sickling
463 [84]. Similarly, we observed alterations in glutathione pathway along with disruptions in
464 glutamine/glutamate metabolism which are the main oxidative damages control system in
465 RBCs of HbS cells.

466 Significant disruptions in glycine, serine, and threonine metabolism with lower 5-
467 aminolevulinate levels (p-value=0.01), which is a by-product of glycine, indicate lower glycine
468 levels (Fig. 3, Fig. S6c). Chronic oxidative stress leads to increased GSSG efflux that exceeds
469 the rate of GSH synthesis [85]. However, rapid efflux of GSSG leads to NADPH depletion
470 which was observed in our study. Thus, de novo GSH synthesis becomes critical in these
471 oxidative stress conditions and needs glycine, glutamate, and cysteine in an ATP-dependent
472 biosynthesis Catabolism of GSH via membrane mounted gamma-glutamyl transpeptidase
473 (GGT) followed by removal of gamma-glutamyl moiety from GSH by gamma-Glutamyl
474 transpeptidase that yields cysteinyl-glycine conjugates (Cys-Gly), and g-glutamyl-amino acid
475 (G-Glu) as products. Hydrolysis of these conjugates by ectoprotein dipeptidases (DPT) yields
476 cysteine and glycine. The g-Glu, glycine and cysteine enter the cell through specific
477 transporters. The g-glutamyl with an amino acid derivative enters the cell and gamma-glutamyl
478 cyclotransferase (G-GCT) converts to 5-oxoproline and the corresponding amino acid. 5-
479 oxoprolinase (OXP) coverts 5-Oxoproline (pyroglutamic acid) to glutamate in a ATP
480 dependent manner. Oxoproline is converted to a dipeptide i.e. g-glutamylcysteine by the
481 combining glutamate and cysteine by the g-glutamylcysteine synthetase (G-GCS) in a two-step
482 reaction which utilizes an ATP per catalytic step. This g-glutamyl cysteine can either act as
483 substrate for GGCT to recycle to 5-oxoproline or it can be converted to GSH by the addition
484 of glycine through GSH sythetase (GS) activity with the usage of an ATP molecule [85-87].

485 ATP production and antioxidant systems within the RBC exploit Hb-based O_2-transport to
486 respond to various physiologic and pathophysiologic stresses. RBCs produce energy through
487 the hexose monophosphate pathway (HMP) and glycolysis, only via the Embden–Meyerhof
488 pathway (EMP), which generates ATP [88]. The HMP route produces NADPH, which powers
489 the thiol-based antioxidant system critical for maintaining homeostasis in the O_2-rich RBC
490 [89]. For example, O_2 offloading promotes glycolysis to generate both 2,3-DPG (a negative
491 allosteric effector of Hb O_2 binding) and ATP. Dynamic regulation of ATP ensures the
492 functional activity of ion pumps, cellular flexibility, drives metabolic reactions and Vaso
493 regulation/dilation under hypoxic stress (Fig. 3). EMP vs. HMP dominance is gated or toggled
494 as a function of the assembly of an EMP protein complex upon the cytoplasmic domain of the

band 3 membrane protein [cdB3, also known as anion exchanger 1 (AE1)] [90-97]. Metabolite flux through EMP vs. HMP oscillates depending on the Hb conformation (oxygenation state) and cdB3 phosphorylation. RBC deoxygenation promotes the generation of ATP, while full oxygenation of RBCs promotes NADPH generation [88, 98]. Rogers and co-workers showed that RBC antioxidant systems fail when HMP flux is blunted by altered cdB3 protein assembly/phosphorylation caused by aberrant Hbs or hypoxia [88, 99, 100].

SS-RBCs are characterized by elevated indices of oxidative stress and depressed ATP levels[101], as well as elevated 2,3-DPG. Recently published evidence suggests a role for pannexin 1 (Px1) in the release of ATP from RBCs due to Gi protein stimulation in SCD [102, 103]. Zhang et al. (2011) identified elevated plasma adenosine as an important determinant of the increased DPG, which may contribute to SCD pathophysiology by decreasing O_2 affinity, which in successive turn promotes HbS polymerization, RBC sickling, and hemolysis [104]. As a consequence, the hydrolysis of extracellular ATP and accumulation of adenosine are favoured, and signalling via adenosine receptors may promote deoxygenation of sickle hemoglobin and in turn (HbS) polymerization and RBC sickling.

The higher levels of pyroglutamic acid or 5-oxoproline in SS-RBCs compared to healthy counterparts can be attributed to an anomaly in salvage pathway of GSH (Fig. S6a, b). 5-oxoproline is acted upon by the 5-oxoprolinase enzyme (ATP-requiring enzyme) to yield glutamate [105]. The conversion of glutamate by the action of two consecutive ATP-dependant enzymes yields back GSH (Fig. 3). However, 5-oxoprolinase has slow and inefficient enzyme activity (reaction rate of 0.45 nmol/h) which may explain the increased levels of 5-oxoproline in the cells[106]. Also, if γ-GCS fails to find an acceptor cysteine during its catalysis, it can autocyclize γ-glutamyl phosphate (intermediate product) to form 5-oxoproline [107].

Furthermore, a depleted pool of ATP, cysteine, and glycine due to sickle pathophysiology as discussed above can retard the activity γ-glutamyl cycle enzymes, i.e., OXP, Y-GCS and GS[108]. Bacchawat et al., proposed a similar futile cycle involving ATP-dependant γ-glutamyl cycle enzymes like γ-GCS and 5-oxoprolinase, leading to rapid depletion of ATP in cystinosis cells per cycle [109].

Alternatively, we can also hypothesize an abnormal activity of GGCT enzyme that leads to the accumulation of 5-oxoproline by acting on g-glutamyl-AA as a response to a decline in the concentration of cellular GSH under oxidative stress. Previous reports showed GGCT reduces oxidative and osmotic stress in RBCs which prevents deformability prolonging their life span [110]. In various cancers, higher GGCT expression was observed and reported as a therapeutic target [111]. In SS-RBCs, a deregulated GGCT response leads to ATP depletion and also limits the availability of glycine and cysteine which are GSH precursors [111].

5. Conclusion

In this study, we reported an altered elemental profile of plasma from sickle cell patients and healthy controls. We observed higher levels of Mg, Zn, Ca, K, and Pb in the plasma of SCD compared to the control groups which corroborated with frequent hemolysis, rampant dehydration of SS-RBCs via ion loss through the Gardos channel (due to K^+ loss), and anemia-induced lead accumulation. Additionally, a steady decrease in plasma Rb/K ratio was observed for SCD when compared to trait and healthy control. We found that compromised functioning of γ-glutamyl cycle leading to high levels of oxidative stress was associated with SCD. These data could be validated in a larger population while taking other clinical parameters into consideration. This will be useful to gain deeper insight into the biomechanical breakdown of SS-RBCs at the molecular level and critical for identifying novel therapeutic targets for SCD patients.

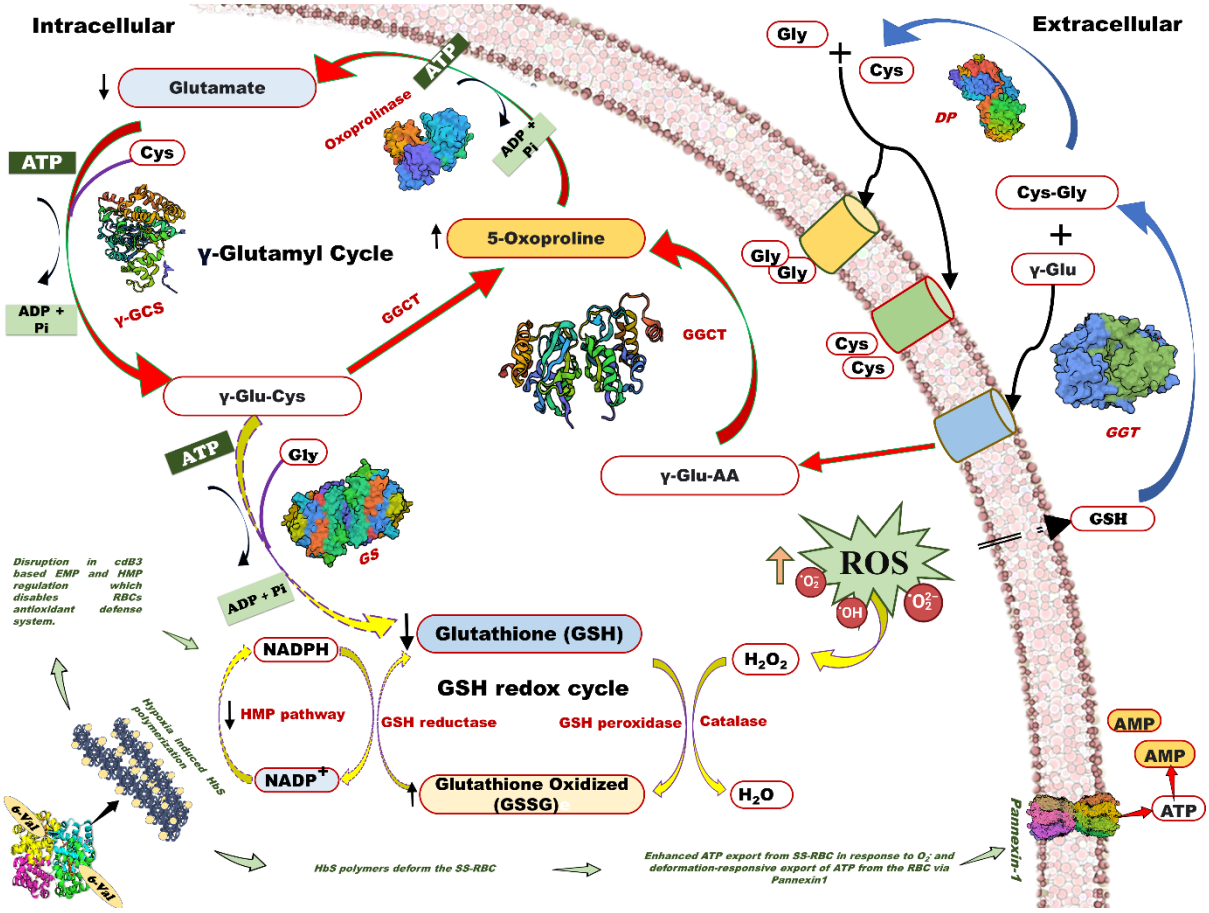

Figure 3. Schematics showing the biomechanical aberration and oxidative stress leading to inoperable γ-glutamyl cycle in SS-RBCs. Metabolites in shades of yellow are increased in SS-RBCs compared to healthy. Metabolites in shades of blue are decreased in SS-RBCs compared to healthy. Increase in color intensity indicates higher magnitude. The solid red arrows indicate an altered gamma-glutamyl cycle; the yellow arrow depicts altered GSH redox cycle; arrows with dashed outline entails an obstructed metabolic reaction; green arrows/text show previously reported pathophysiology of SS-RBCs. GGCT: gamma-glutamyl cyclotransferase; GGT: gamma-glutamyltranspeptidase; γ-GCS: glutamate cysteine ligase; GS: glutathione synthase; OXP: 5-oxoprolinase; γ-Glu-Cys-Gly: glutathione; DP: dipeptidase; HMP: hexose monophosphate pathway; EMP: Embden Meyerhof pathway; ATP: Adenosine triphosphate; ADP: Adenosine diphosphate; AMP: Adenosine monophosphate; Pi: phosphate.

Funding information

SK acknowledges the financial support from DBT, Government of India through extramural projects [BT/PR8391/BRB/10/1231/2013; BT/COE/34/SP15246/2015 and BT/PR13531/MED/30/1523/ 2015]. S Kundu also acknowledges financial support from the University of Delhi (R & D Grant; Institution of Eminence grant IOE/FRP/LS/2020/ 27); UGC, Government of India (SAP program) and DST, Government of India (PURSE Program). RN acknowledges Core support from the ICGEB New Delhi Component and project support from Department of Biotechnology New Delhi. SB acknowledges Department of Biotechnology, Government of India for Research Fellowships, ASR is thankful to the Government of Odisha for the Biju Patnaik Research Fellowship.

Author contributions

Shruti Bhatt: Designed and performed ionomic and metabolomic experiments, analysed and plotted data, wrote manuscript.

Amit Kumar Mohapatra: performed ionomic experiments, analysed ionomics data, wrote manuscript

Satyabrata Meher: recruitment of participants, clinical profiling, sample collection and transport

Apratim Sai Rajesh: recruitment of participants, clinical profiling, sample collection and transport

Pradip Kumar Panda: recruitment of participants, clinical profiling, sample collection and transport

Ranjan Kumar Nanda: conceived and supervised the study, analysed data, provided tools and reagents, and wrote the manuscript.

Suman Kundu: conceived and supervised the study, analysed data, provided tools and reagents, and wrote the manuscript.

Conflicts of interest

The authors declare no conflict of interest.

Acknowledgement

Prof. Alo Nag is acknowledged for administrative supervision and scientific discussion with SB. Ms. Nidhi Mittal is acknowledged for scientific discussions with SB. Central Instrumentation Facility (CIF), Delhi University, is appreciated for help with metabolomics data collection spectra data collection. Anil Bhansali and Dharmender Singh for miscellaneous help to the laboratory.

References

[1] L. Pauling, H.A. Itano, et al., Sickle cell anemia a molecular disease, Science 110(2865) (1949) 543-8.

[2] S.A. Pereira, S. Brener, C.S. Cardoso, A.B. Proietti, Sickle Cell Disease: quality of life in patients with hemoglobin SS and SC disorders, Rev Bras Hematol Hemoter 35(5) (2013) 325-31.

[3] F.B. Piel, [Sickle-cell disease: geographical distribution and population estimates], Med Sci (Paris) 29(11) (2013) 965-7.

[4] F.B. Piel, M.H. Steinberg, D.C. Rees, Sickle Cell Disease, N Engl J Med 376(16) (2017) 1561-1573.

[5] F.B. Piel, T.N. Williams, Subphenotypes of sickle cell disease in Africa, Blood 130(20) (2017) 2157-2158.

[6] D.C. Rees, T.N. Williams, M.T. Gladwin, Sickle-cell disease, Lancet 376(9757) (2010) 2018-31.

[7] M.K. Safo, O. Abdulmalik, R. Danso-Danquah, J.C. Burnett, S. Nokuri, G.S. Joshi, F.N. Musayev, T. Asakura, D.J. Abraham, Structural basis for the potent antisickling effect of a novel class of five-membered heterocyclic aldehydic compounds, J Med Chem 47(19) (2004) 4665-76.

[8] M.H. Steinberg, Sickle cell anemia, the first molecular disease: overview of molecular etiology, pathophysiology, and therapeutic approaches, ScientificWorldJournal 8 (2008) 1295-324.

[9] J.F. Bertles, R. Rabinowitz, J. Dobler, Hemoglobin interaction: modification of solid phase composition in the sickling phenomenon, Science 169(3943) (1970) 375-7.

[10] S. Ballas, Sickle cell pain: Second edition, 2015.

[11] S.K. Ballas, D.S. Darbari, Review/overview of pain in sickle cell disease, Complement Ther Med 49 (2020) 102327.

[12] A. Sanyaolu, E. Agiri, C. Bertram, L. Brookes, J. Choudhury, D. Datt, A. Ibrahim, A. Maciejko, A. Mansfield, J. Nkrumah, M. Williams, Current modalities of sickle cell disease management, Blood Sci 2(4) (2020) 109-116.

[13] P. Sundd, M.T. Gladwin, E.M. Novelli, Pathophysiology of Sickle Cell Disease, Annu Rev Pathol 14 (2019) 263-292.

[14] B.P. Yawn, G.R. Buchanan, A.N. Afenyi-Annan, S.K. Ballas, K.L. Hassell, A.H. James, L. Jordan, S.M. Lanzkron, R. Lottenberg, W.J. Savage, P.J. Tanabe, R.E. Ware, M.H. Murad, J.C. Goldsmith, E. Ortiz, R. Fulwood, A. Horton, J. John-Sowah, Management of sickle cell disease: summary of the 2014 evidence-based report by expert panel members, JAMA 312(10) (2014) 1033-48.

[15] H. Tran, M. Gupta, K. Gupta, Targeting novel mechanisms of pain in sickle cell disease, Blood 130(22) (2017) 2377-2385.

[16] R. Culp-Hill, A.J. Srinivasan, S. Gehrke, R. Kamyszek, A. Ansari, N. Shah, I. Welsby, A. D'Alessandro, Effects of red blood cell (RBC) transfusion on sickle cell disease recipient plasma and RBC metabolism, Transfusion 58(12) (2018) 2797-2806.

[17] A. D'Alessandro, S.M. Nouraie, Y. Zhang, F. Cendali, F. Gamboni, J.A. Reisz, X. Zhang, K.W. Bartsch, M.D. Galbraith, V.R. Gordeuk, M.T. Gladwin, In vivo evaluation of the effect of sickle cell hemoglobin S, C and therapeutic transfusion on erythrocyte metabolism and cardiorenal dysfunction, Am J Hematol (2023).

[18] K.C. Dembele, T. Mintz, C. Veyrat-Durebex, F. Chabrun, S. Chupin, L. Tessier, G. Simard, D. Henrion, D. Mirebeau-Prunier, J.M. Chao de la Barca, P.L. Tharaux, P. Reynier, Metabolomic Profiling of Plasma and Erythrocytes in Sickle Mice Points to Altered Nociceptive Pathways, Cells 9(6) (2020).

[19] S.R. Goodman, B.S. Pace, K.C. Hansen, A. D'Alessandro, Y. Xia, O. Daescu, S.J. Glatt, Minireview: Multiomic candidate biomarkers for clinical manifestations of sickle cell severity: Early steps to precision medicine, Exp Biol Med (Maywood) 241(7) (2016) 772-81.

[20] A.L. Okwi, M. Ocaido, W. Byarugaba, C.M. Ndugwa, A. Parkes, Sickling and solubility tests and the peripheral blood film method for screening for sickle cell disease. [corrected], S Afr Med J 99(12) (2009) 887-91.

[21] Z. Pang, G. Zhou, J. Ewald, L. Chang, O. Hacariz, N. Basu, J. Xia, Using MetaboAnalyst 5.0 for LC-HRMS spectra processing, multi-omics integration and covariate adjustment of global metabolomics data, Nat Protoc 17(8) (2022) 1735-1761.

[22] G. Bosman, Disturbed Red Blood Cell Structure and Function: An Exploration of the Role of Red Blood Cells in Neurodegeneration, Front Med (Lausanne) 5 (2018) 198.

[23] E. Szczesny-Malysiak, J. Dybas, A. Blat, K. Bulat, K. Kus, M. Kaczmarska, A. Wajda, K. Malek, S. Chlopicki, K.M. Marzec, Irreversible alterations in the hemoglobin structure affect oxygen binding in human packed red blood cells, Biochim Biophys Acta Mol Cell Res 1867(11) (2020) 118803.
[24] G. Tomaiuolo, Biomechanical properties of red blood cells in health and disease towards microfluidics, Biomicrofluidics 8(5) (2014) 051501.
[25] N. Cilek, E. Ugurel, E. Goksel, O. Yalcin, Signaling mechanisms in red blood cells: A view through the protein phosphorylation and deformability, J Cell Physiol (2023).
[26] H. Li, G. Lykotrafitis, Erythrocyte membrane model with explicit description of the lipid bilayer and the spectrin network, Biophys J 107(3) (2014) 642-653.
[27] V. Pretini, M.H. Koenen, L. Kaestner, M. Fens, R.M. Schiffelers, M. Bartels, R. Van Wijk, Red Blood Cells: Chasing Interactions, Front Physiol 10 (2019) 945.
[28] S.L. Spitalnik, D.V. Devine, Translating red cell "omics" into new perspectives in transfusion medicine: mining the gems in the data mountains, Transfusion 59(1) (2019) 2-5.
[29] C. Tang, Q. Meng, K. Zhang, T. Zhan, Q. Zhao, S. Zhang, J. Zhang, Multi-omics analyses of red blood cell reveal antioxidation mechanisms associated with hemolytic toxicity of gossypol, Oncotarget 8(61) (2017) 103693-103709.
[30] A. Iolascon, I. Andolfo, R. Russo, Advances in understanding the pathogenesis of red cell membrane disorders, Br J Haematol 187(1) (2019) 13-24.
[31] M. Cascella, S. Vaqar, Hypermagnesemia, StatPearls, Treasure Island (FL), 2023.
[32] A.O. Olukoga, H.O. Adewoye, R.T. Erasmus, M.A. Adedoyin, Erythrocyte and plasma magnesium in sickle-cell anaemia, East Afr Med J 67(5) (1990) 348-54.
[33] A.O. Olukoga, R.T. Erasmus, H.O. Adewoye, Erythrocyte and plasma magnesium status in Nigerians with diabetes mellitus, Ann Clin Biochem 26 (Pt 1) (1989) 74-7.
[34] C. Antwi-Boasiako, Y.A. Kusi-Mensah, C. Hayfron-Benjamin, R. Aryee, G.B. Dankwah, L.A. Kwawukume, E.O. Darkwa, Total Serum Magnesium Levels and Calcium-To-Magnesium Ratio in Sickle Cell Disease, Medicina (Kaunas) 55(9) (2019).
[35] O.O. Yousif, M.K. Hassan, L.M. Al-Naama, Red Blood Cell and Serum Magnesium Levels Among Children and Adolescents With Sickle Cell Anemia, Biol Trace Elem Res 186(2) (2018) 295-304.
[36] B.F. Cameron, P. Smariga, Calcium exchange and calcium-related effects in normal and sickle cell anemia erythrocytes, Prog Clin Biol Res 20 (1978) 105-22.
[37] V. Malinovska, P. Matonoha, V. D'Andrea, L. Malinovsky, A. Zechmeister, [The role of calcium in the effect of stress hormones], Cas Lek Cesk 130(22-23) (1991) 631-4.
[38] A. Bogdanova, A. Makhro, J. Wang, P. Lipp, L. Kaestner, Calcium in red blood cells-a perilous balance, Int J Mol Sci 14(5) (2013) 9848-72.
[39] L. Hertz, R. Huisjes, E. Llaudet-Planas, P. Petkova-Kirova, A. Makhro, J.G. Danielczok, S. Egee, M. Del Mar Manu-Pereira, R. van Wijk, J.L. Vives Corrons, A. Bogdanova, L. Kaestner, Is Increased Intracellular Calcium in Red Blood Cells a Common Component in the Molecular Mechanism Causing Anemia?, Front Physiol 8 (2017) 673.
[40] C. Brugnara, L. de Franceschi, S.L. Alper, Inhibition of Ca(2+)-dependent K+ transport and cell dehydration in sickle erythrocytes by clotrimazole and other imidazole derivatives, J Clin Invest 92(1) (1993) 520-6.
[41] C. Brugnara, D.C. Tosteson, Inhibition of K transport by divalent cations in sickle erythrocytes, Blood 70(6) (1987) 1810-5.
[42] E. Nader, M. Romana, P. Connes, The Red Blood Cell-Inflammation Vicious Circle in Sickle Cell Disease, Front Immunol 11 (2020) 454.
[43] V. Barodka, J.G. Mohanty, A.K. Mustafa, L. Santhanam, A. Nyhan, A.K. Bhunia, G. Sikka, D. Nyhan, D.E. Berkowitz, J.M. Rifkind, Nitroprusside inhibits calcium-induced impairment of red blood cell deformability, Transfusion 54(2) (2014) 434-44.
[44] C. Antwi-Boasiako, Y.A. Kusi-Mensah, C. Hayfron-Benjamin, R. Aryee, G.B. Dankwah, K.L. Abla, E. Owusu Darkwa, F.A. Botchway, E. Sampene-Donkor, Serum Potassium, Sodium, and Chloride Levels in Sickle Cell Disease Patients and Healthy Controls: A Case-Control Study at Korle-Bu Teaching Hospital, Accra, Biomark Insights 14 (2019) 1177271919873889.

[45] S. Pandey, A. Sharma, S. Dahia, V. Shah, V. Sharma, R.M. Mishra, S. Pandey, R. Saxena, Biochemical indicator of sickle cell disease: preliminary report from India, Indian J Clin Biochem 27(2) (2012) 191-5.
[46] C.T. Noguchi, A.N. Schechter, G.P. Rodgers, Sickle cell disease pathophysiology, Baillieres Clin Haematol 6(1) (1993) 57-91.
[47] D. Manwani, P.S. Frenette, Vaso-occlusion in sickle cell disease: pathophysiology and novel targeted therapies, Blood 122(24) (2013) 3892-8.
[48] J.R. Aluoch, Renal and electrolyte profile in steady state sickle cell disease: observations in patients with sickle cell disease in The Netherlands, Trop Geogr Med 41(2) (1989) 128-32.
[49] J.R. Asirvatham, V. Moses, L. Bjornson, Errors in potassium measurement: a laboratory perspective for the clinician, N Am J Med Sci 5(4) (2013) 255-9.
[50] S. Tomlinson, P.D. Mathialagan, S.K. Maloney, Special K: testing the potassium link between radioactive rubidium (86Rb) turnover and metabolic rate, J Exp Biol 217(Pt 7) (2014) 1040-5.
[51] H.L. Meltzer, R.M. Taylor, S.R. Platmann, R.R. Fieve, Rubidium: a potential modifier of affect and behaviour, Nature 223(5203) (1969) 321-2.
[52] N. Rahimi, M. Hassanipour, F. Yarmohammadi, H. Faghir-Ghanesefat, N. Pourshadi, E. Bahramnejad, A.R. Dehpour, Nitric oxide and glutamate are contributors of anti-seizure activity of rubidium chloride: A comparison with lithium, Neurosci Lett 708 (2019) 134349.
[53] L. Xiao, G. Zan, J. Qin, X. Wei, G. Lu, X. Li, H. Zhang, Y. Zou, L. Yang, M. He, Z. Zhang, X. Yang, Combined exposure to multiple metals and cognitive function in older adults, Ecotoxicol Environ Saf 222 (2021) 112465.
[54] N. Kordjazy, A. Haj-Mirzaian, S. Amiri, S. Ostadhadi, M. Kordjazy, M. Sharifzadeh, A.R. Dehpour, Elevated level of nitric oxide mediates the anti-depressant effect of rubidium chloride in mice, Eur J Pharmacol 762 (2015) 411-8.
[55] S. Martin, M.C. Roderick, C. Abel, P. Wolters, M.A. Toledo-Tamula, C. Fitzhugh, M. Hsieh, J. Tisdale, Neurocognitive functioning in symptomatic adults with sickle cell disease: A description and comparison with unaffected siblings, Neuropsychol Rehabil 30(9) (2020) 1666-1681.
[56] C.T. Hijmans, K. Fijnvandraat, M.A. Grootenhuis, N. van Geloven, H. Heijboer, M. Peters, J. Oosterlaan, Neurocognitive deficits in children with sickle cell disease: a comprehensive profile, Pediatr Blood Cancer 56(5) (2011) 783-8.
[57] S.K. Ballas, Neurocognitive complications of sickle cell anemia in adults, JAMA 303(18) (2010) 1862-3.
[58] L.O. Matondo, E. Kija, K.P. Manji, Neurocognitive Functioning among Children with Sickle Cell Anemia Attending SCA Clinic at MNH, Dar es Salaam, Tanzania, Neurol Res Int 2020 (2020) 3636547.
[59] N.S. Green, D. Munube, P. Bangirana, L.R. Buluma, B. Kebirungi, R. Opoka, E. Mupere, P. Kasirye, S. Kiguli, A. Birabwa, M.S. Kawooya, S.K. Lubowa, R. Sekibira, E. Kayongo, H. Hume, M. Elkind, W. Peng, G. Li, C. Rosano, P. LaRussa, F.J. Minja, A. Boehme, R. Idro, Burden of neurological and neurocognitive impairment in pediatric sickle cell anemia in Uganda (BRAIN SAFE): a cross-sectional study, BMC Pediatr 19(1) (2019) 381.
[60] A.A. Hegazy, M.M. Zaher, M.A. Abd El-Hafez, A.A. Morsy, R.A. Saleh, Relation between anemia and blood levels of lead, copper, zinc and iron among children, BMC Res Notes 3 (2010) 133.
[61] M.M. Lubran, Lead toxicity and heme biosynthesis, Ann Clin Lab Sci 10(5) (1980) 402-13.
[62] J. Schwartz, P.J. Landrigan, E.L. Baker, Jr., W.A. Orenstein, I.H. von Lindern, Lead-induced anemia: dose-response relationships and evidence for a threshold, Am J Public Health 80(2) (1990) 165-8.
[63] C.G. Drossos, K.T. Mavroidis, Z. Papadopoulou-Daifotis, D.N. Michalodimitrakis, L.X. Salamalikis, A.K. Gounaris, D.D. Varonos, Environmental lead pollution in Greece, Am Ind Hyg Assoc J 43(10) (1982) 796-8.
[64] I.H. Elkhidir, S.S. Ali, W.K. Ali, H.R. Madani, R.A. Basheir, R.M. Altayeb, R.H.S. Shazali, S. Fadlelmoula, W.M. Eltayeb, Z.I. Omar, M. Elnil, S.O.O. Mohamed, Zinc, Magnesium, and Copper Levels in Patients with Sickle Cell Disease: A Systematic Review and Meta-analysis, Avicenna J Med 12(2) (2022) 45-53.
[65] R. Hasanato, Alterations in serum levels of copper, zinc, and selenium among children with sickle cell anemia, Turk J Med Sci 49(5) (2019) 1287-1291.

[66] A. Ece, B.S. Uyanik, A. Iscan, P. Ertan, M.R. Yigitoglu, Increased serum copper and decreased serum zinc levels in children with iron deficiency anemia, Biol Trace Elem Res 59(1-3) (1997) 31-9.
[67] S. Turgut, A. Polat, M. Inan, G. Turgut, G. Emmungil, M. Bican, T.Y. Karakus, O. Genc, Interaction between anemia and blood levels of iron, zinc, copper, cadmium and lead in children, Indian J Pediatr 74(9) (2007) 827-30.
[68] I.J. Newhouse, D.B. Clement, C. Lai, Effects of iron supplementation and discontinuation on serum copper, zinc, calcium, and magnesium levels in women, Med Sci Sports Exerc 25(5) (1993) 562-71.
[69] H.C. Kim, N.P. Dugan, J.H. Silber, M.B. Martin, E. Schwartz, K. Ohene-Frempong, A.R. Cohen, Erythrocytapheresis therapy to reduce iron overload in chronically transfused patients with sickle cell disease, Blood 83(4) (1994) 1136-42.
[70] K.R. Rao, A.R. Patel, P. McGinnis, M.K. Patel, Iron stores in adults with sickle cell anemia, J Lab Clin Med 103(5) (1984) 792-7.
[71] L. Flohe, W.A. Gunzler, H.H. Schock, Glutathione peroxidase: a selenoenzyme, FEBS Lett 32(1) (1973) 132-4.
[72] J.T. Rotruck, A.L. Pope, H.E. Ganther, A.B. Swanson, D.G. Hafeman, W.G. Hoekstra, Selenium: biochemical role as a component of glutathione peroxidase, Science 179(4073) (1973) 588-90.
[73] S. Li, W. Sun, K. Zhang, J. Zhu, X. Jia, X. Guo, Q. Zhao, C. Tang, J. Yin, J. Zhang, Selenium deficiency induces spleen pathological changes in pigs by decreasing selenoprotein expression, evoking oxidative stress, and activating inflammation and apoptosis, J Anim Sci Biotechnol 12(1) (2021) 65.
[74] G.F. Combs, Jr., W.P. Gray, Chemopreventive agents: selenium, Pharmacol Ther 79(3) (1998) 179-92.
[75] R. Irons, B.A. Carlson, D.L. Hatfield, C.D. Davis, Both selenoproteins and low molecular weight selenocompounds reduce colon cancer risk in mice with genetically impaired selenoprotein expression, J Nutr 136(5) (2006) 1311-7.
[76] R. Scott, A. MacPherson, R.W. Yates, B. Hussain, J. Dixon, The effect of oral selenium supplementation on human sperm motility, Br J Urol 82(1) (1998) 76-80.
[77] M.P. Look, J.K. Rockstroh, G.S. Rao, K.A. Kreuzer, S. Barton, H. Lemoch, T. Sudhop, J. Hoch, K. Stockinger, U. Spengler, T. Sauerbruch, Serum selenium, plasma glutathione (GSH) and erythrocyte glutathione peroxidase (GSH-Px)-levels in asymptomatic versus symptomatic human immunodeficiency virus-1 (HIV-1)-infection, Eur J Clin Nutr 51(4) (1997) 266-72.
[78] L. Kiremidjian-Schumacher, M. Roy, Effect of selenium on the immunocompetence of patients with head and neck cancer and on adoptive immunotherapy of early and established lesions, Biofactors 14(1-4) (2001) 161-8.
[79] C.R. Morris, J.H. Suh, W. Hagar, S. Larkin, D.A. Bland, M.H. Steinberg, E.P. Vichinsky, M. Shigenaga, B. Ames, F.A. Kuypers, E.S. Klings, Erythrocyte glutamine depletion, altered redox environment, and pulmonary hypertension in sickle cell disease, Blood 111(1) (2008) 402-10.
[80] E. Nur, B.J. Biemond, H.M. Otten, D.P. Brandjes, J.J. Schnog, C.S. Group, Oxidative stress in sickle cell disease; pathophysiology and potential implications for disease management, Am J Hematol 86(6) (2011) 484-9.
[81] S.R. Goodman, The irreversibly sickled cell: a perspective, Cell Mol Biol (Noisy-le-grand) 50(1) (2004) 53-8.
[82] M. Aslan, D. Thornley-Brown, B.A. Freeman, Reactive species in sickle cell disease, Ann N Y Acad Sci 899 (2000) 375-91.
[83] F.Q. Schafer, G.R. Buettner, Redox environment of the cell as viewed through the redox state of the glutathione disulfide/glutathione couple, Free Radic Biol Med 30(11) (2001) 1191-212.
[84] M.C. Garel, C. Domenget, J. Caburi-Martin, C. Prehu, F. Galacteros, Y. Beuzard, Covalent binding of glutathione to hemoglobin. I. Inhibition of hemoglobin S polymerization, J Biol Chem 261(31) (1986) 14704-9.
[85] M. Reid, A. Badaloo, T. Forrester, F. Jahoor, In vivo rates of erythrocyte glutathione synthesis in adults with sickle cell disease, Am J Physiol Endocrinol Metab 291(1) (2006) E73-9.
[86] R. Franco, O.J. Schoneveld, A. Pappa, M.I. Panayiotidis, The central role of glutathione in the pathophysiology of human diseases, Arch Physiol Biochem 113(4-5) (2007) 234-58.
[87] J.E. Snoke, K. Bloch, Studies on the mechanism of action of glutathione synthetase, J Biol Chem 213(2) (1955) 825-35.

[88] S.C. Rogers, A. Said, D. Corcuera, D. McLaughlin, P. Kell, A. Doctor, Hypoxia limits antioxidant capacity in red blood cells by altering glycolytic pathway dominance, FASEB J 23(9) (2009) 3159-70.
[89] W.G. Siems, O. Sommerburg, T. Grune, Erythrocyte free radical and energy metabolism, Clin Nephrol 53(1 Suppl) (2000) S9-17.
[90] P.S. Low, P. Rathinavelu, M.L. Harrison, Regulation of glycolysis via reversible enzyme binding to the membrane protein, band 3, J Biol Chem 268(20) (1993) 14627-31.
[91] I. Messana, M. Orlando, L. Cassiano, L. Pennacchietti, C. Zuppi, M. Castagnola, B. Giardina, Human erythrocyte metabolism is modulated by the O2-linked transition of hemoglobin, FEBS Lett 390(1) (1996) 25-8.
[92] D. Sterling, R.A. Reithmeier, J.R. Casey, A transport metabolon. Functional interaction of carbonic anhydrase II and chloride/bicarbonate exchangers, J Biol Chem 276(51) (2001) 47886-94.
[93] L.J. Bruce, R. Beckmann, M.L. Ribeiro, L.L. Peters, J.A. Chasis, J. Delaunay, N. Mohandas, D.J. Anstee, M.J. Tanner, A band 3-based macrocomplex of integral and peripheral proteins in the RBC membrane, Blood 101(10) (2003) 4180-8.
[94] N.N. Barvitenko, N.C. Adragna, R.E. Weber, Erythrocyte signal transduction pathways, their oxygenation dependence and functional significance, Cell Physiol Biochem 15(1-4) (2005) 1-18.
[95] M.E. Campanella, H. Chu, P.S. Low, Assembly and regulation of a glycolytic enzyme complex on the human erythrocyte membrane, Proc Natl Acad Sci U S A 102(7) (2005) 2402-7.
[96] H. Chu, P.S. Low, Mapping of glycolytic enzyme-binding sites on human erythrocyte band 3, Biochem J 400(1) (2006) 143-51.
[97] H. Chu, A. Breite, P. Ciraolo, R.S. Franco, P.S. Low, Characterization of the deoxyhemoglobin binding site on human erythrocyte band 3: implications for O2 regulation of erythrocyte properties, Blood 111(2) (2008) 932-8.
[98] B.S. Kirby, G. Hanna, H.C. Hendargo, T.J. McMahon, Restoration of intracellular ATP production in banked red blood cells improves inducible ATP export and suppresses RBC-endothelial adhesion, Am J Physiol Heart Circ Physiol 307(12) (2014) H1737-44.
[99] S.C. Rogers, J.G. Ross, A. d'Avignon, L.B. Gibbons, V. Gazit, M.N. Hassan, D. McLaughlin, S. Griffin, T. Neumayr, M. Debaun, M.R. DeBaun, A. Doctor, Sickle hemoglobin disturbs normal coupling among erythrocyte O2 content, glycolysis, and antioxidant capacity, Blood 121(9) (2013) 1651-62.
[100] E. Ferru, K. Giger, A. Pantaleo, E. Campanella, J. Grey, K. Ritchie, R. Vono, F. Turrini, P.S. Low, Regulation of membrane-cytoskeletal interactions by tyrosine phosphorylation of erythrocyte band 3, Blood 117(22) (2011) 5998-6006.
[101] R.L. Sabina, N.J. Wandersee, C.A. Hillery, Ca2+-CaM activation of AMP deaminase contributes to adenine nucleotide dysregulation and phosphatidylserine externalization in human sickle erythrocytes, Br J Haematol 144(3) (2009) 434-45.
[102] M.F. Leal Denis, J.J. Incicco, M.V. Espelt, S.V. Verstraeten, O.P. Pignataro, E.R. Lazarowski, P.J. Schwarzbaum, Kinetics of extracellular ATP in mastoparan 7-activated human erythrocytes, Biochim Biophys Acta 1830(10) (2013) 4692-707.
[103] B.S. Kirby, M.A. Sparks, E.R. Lazarowski, D.A. Lopez Domowicz, H. Zhu, T.J. McMahon, Pannexin 1 channels control the hemodynamic response to hypoxia by regulating O(2)-sensitive extracellular ATP in blood, Am J Physiol Heart Circ Physiol 320(3) (2021) H1055-H1065.
[104] H. Zhu, R. Zennadi, B.X. Xu, J.P. Eu, J.A. Torok, M.J. Telen, T.J. McMahon, Impaired adenosine-5'-triphosphate release from red blood cells promotes their adhesion to endothelial cells: a mechanism of hypoxemia after transfusion, Crit Care Med 39(11) (2011) 2478-86.
[105] P. Van der Werf, M. Orlowski, A. Meister, Enzymatic conversion of 5-oxo-L-proline (L-pyrrolidone carboxylate) to L-glutamate coupled with cleavage of adenosine triphosphate to adenosine diphosphate, a reaction in the -glutamyl cycle, Proc Natl Acad Sci U S A 68(12) (1971) 2982-5.
[106] M. Watanabe, M. Kusano, A. Oikawa, A. Fukushima, M. Noji, K. Saito, Physiological roles of the beta-substituted alanine synthase gene family in Arabidopsis, Plant Physiol 146(1) (2008) 310-20.
[107] J.J. Abbott, J. Pei, J.L. Ford, Y. Qi, V.N. Grishin, L.A. Pitcher, M.A. Phillips, N.V. Grishin, Structure prediction and active site analysis of the metal binding determinants in gamma -glutamylcysteine synthetase, J Biol Chem 276(45) (2001) 42099-107.
[108] P.G. Richman, A. Meister, Regulation of gamma-glutamyl-cysteine synthetase by nonallosteric feedback inhibition by glutathione, J Biol Chem 250(4) (1975) 1422-6.

[109] A.K. Bachhawat, S. Yadav, The glutathione cycle: Glutathione metabolism beyond the gamma-glutamyl cycle, IUBMB Life 70(7) (2018) 585-592.
[110] Z. He, X. Sun, S. Wang, D. Bai, X. Zhao, Y. Han, P. Hao, X.S. Liu, Ggct (gamma-glutamyl cyclotransferase) plays an important role in erythrocyte antioxidant defense and red blood cell survival, Br J Haematol 195(2) (2021) 267-275.
[111] S. Kageyama, E. Hanada, H. Ii, K. Tomita, T. Yoshiki, A. Kawauchi, Gamma-Glutamylcyclotransferase: A Novel Target Molecule for Cancer Diagnosis and Treatment, Biomed Res Int 2015 (2015) 345219.